

Nanoscale

Accepted Manuscript



This is an *Accepted Manuscript*, which has been through the Royal Society of Chemistry peer review process and has been accepted for publication.

Accepted Manuscripts are published online shortly after acceptance, before technical editing, formatting and proof reading. Using this free service, authors can make their results available to the community, in citable form, before we publish the edited article. We will replace this *Accepted Manuscript* with the edited and formatted *Advance Article* as soon as it is available.

You can find more information about *Accepted Manuscripts* in the [Information for Authors](#).

Please note that technical editing may introduce minor changes to the text and/or graphics, which may alter content. The journal's standard [Terms & Conditions](#) and the [Ethical guidelines](#) still apply. In no event shall the Royal Society of Chemistry be held responsible for any errors or omissions in this *Accepted Manuscript* or any consequences arising from the use of any information it contains.

Coiled fiber scaffolds embedded with gold nanoparticles improve the performance of engineered cardiac tissues

Sharon Fleischer^{a,b,†}, Michal Shevach^{a,b,†}, Ron Feiner^{a,b,†}, Tal Dvir^{a,b,c,*}

^aThe Laboratory for Tissue Engineering and Regenerative Medicine, Department of Molecular Microbiology and Biotechnology, George S. Wise Faculty of Life Science, Tel Aviv University, Tel Aviv 69978, Israel.

^bThe Center for Nanoscience and Nanotechnology, Tel Aviv University, Tel Aviv 69978, Israel.

^cDepartment of Materials Science and Engineering, Faculty of Engineering, Tel Aviv University, Tel Aviv 69978, Israel.

*Corresponding author: tdvir@post.tau.ac.il

†Equal contribution

Key words: Cardiac tissue engineering, coiled fibers, electrospinning, gold nanoparticles, scaffolds

Introduction

One of every three deaths in the United States is caused by cardiovascular diseases.¹ Myocardial infarction (MI) captures a significant part of these diseases, and is associated with significant morbidity and mortality.² To date, strategies such as cell therapy, where cells are injected directly to the infarct, have been developed to repopulate the scar tissue with contracting cells.^{3,4} However, most of these strategies have shown limited success in sustaining the cells at the area of the infarct.^{5,6} Cardiac tissue engineering is a promising strategy for promoting heart regeneration.⁷⁻⁹ In this approach, cells are grown within three-dimensional (3D) biomaterials to promote their organization into contracting cardiac patches.¹⁰⁻¹⁵ Later on these patches can be implanted on the diseased heart to regain function.^{16,17} For successful cell assembly, integration and repair, the 3D scaffold supporting the cells should promote rapid electrical coupling between cardiac muscle cells and allow the forming cell bundles to extend and contract efficiently.^{18,19} To improve cell-cell coupling at the electrical level we have recently reported that cardiac cells can interact with each other through gold nanowires¹¹ or spherical nanoparticles.²⁰ These nanostructures were incorporated within 3D macroporous or electrospun scaffolds to form hybrid nanocomposite scaffolds. Cardiac tissues grown within these scaffolds exhibited anisotropic transfer of the electrical signal leading to higher contraction rates and stronger contraction forces.^{11,20}

Although synchronous contraction was observed throughout these engineered cardiac patches, the microenvironment in which the tissues were engineered lacked mechanical properties of the natural microenvironment. These properties are essential for efficient

tissue contraction and relaxation. The natural heart matrix contains a unique subpopulation of coiled perimysial fibers.²¹ These fibers stretch and re-coil with the heart muscle, providing it with unique mechanical properties crucial for its efficient and continuous contractions.^{21,22} Recently, we reported on the importance of recapitulating these fibers for engineering functional cardiac tissues.²³ Cardiac tissues grown within these coiled-fiber scaffolds exhibited stronger contraction forces, higher beating rates and lower excitation thresholds than tissues grown within straight fiber scaffolds.²³

Here we sought to further improve cardiac patch performances by integration of gold nanoparticles (AuNPs) ensuring anisotropic transfer of the electrical signal throughout engineered cardiac tissues, with coiled fiber scaffolds. Fig. 1 schematically illustrates the experimental process. Poly(ϵ -caprolactone) (PCL) was dissolved in a 1:1 ratio of dichloromethane (DCM) and dimethylformamide (DMF), and electrospun on a static collector to fabricate coiled fibers. The fibers were then placed in a VST e-beam evaporator and Au was deposited on their surface to create the nanocomposite coiled fiber scaffolds.

Inspired by the structure of natural coiled perimysial fibers (Fig. 2A), we synthetically fabricated similar coiled electrospun fibers (Fig. 2B). Scaffolds composed of such coiled fibers with diameters ranging between a few hundreds of nanometers to several micrometers exhibited an average pore area $> 4000 \mu\text{m}^2$ (Fig. 2C,D).²³ We next sought to overcome the limited ability of the scaffolds to propagate the electrical signal between cultured cardiac cells by evaporating AuNPs with a nominal thickness of 10 nm

onto the surface of the fibers. ESEM images revealed that AuNPs were homogeneously distributed on the surface of the fibers (Fig. 2E). Elemental mapping using energy dispersive x-ray spectroscopy (EDX) confirmed that the scaffolds were covered with AuNPs (Fig. 2F).

Recently it was reported that modification of silk electrospun fibers with AuNPs altered their mechanical properties.²⁴ To investigate the effect of the AuNPs on the coiled fibers, single fibers were electrospun on slides and the z-axis-Young's modulus of fibers with and without AuNPs was investigated using atomic force microscope (AFM). Fig. 3A and 3B revealed the topography of fibers with and without AuNPs. While the pristine fibers were relatively smooth, the AuNPs were clearly seen on the surface of the modified fibers. This allowed a relatively easy placement of the AFM tip on the AuNPs for measuring the mechanical properties of the composite fibers. As shown, the AuNPs significantly increased the elastic modulus of the fibers (Fig. 3B; $p= 0.008$). Measuring fiber stiffness in the longitudinal direction by Lloyd mechanical tester revealed no change (data not shown).

Next, we investigated the potential of the AuNPs-coiled fiber scaffolds (AuNPs scaffolds) to induce cardiac cell assembly into a mature tissue with morphological and biochemical hallmarks resembling those of the natural myocardium. We and others have previously shown that engineered cardiac tissue function can be improved by incorporation of gold nanostructures into macroporous scaffolds, hydrogels or straight fibers.^{11, 20, 25} In this study, we sought to explore the potential of AuNPs to improve the structural and

functional assembly of cardiac tissues grown within coiled fiber scaffolds. Cardiac cells were isolated from neonatal rats and cultured for 7 days within pristine or AuNPs scaffolds. On day 7, engineered cardiac tissues were stained for α -sarcomeric actinin, a marker associated with cardiac muscle contraction. Fig. 4A revealed that cardiac cells cultured within pristine scaffolds exhibited limited cell spreading and a rounded morphology. Furthermore, massive cell-cell interactions were not observed and cardiac cell bundles were not formed. In contrast, cardiac cells cultured within AuNPs scaffolds exhibited aligned and elongated morphology with massive actinin striation (Fig. 4B). The cells organized into elongated and aligned cardiac-cell bundles, resembling the natural morphology of cell bundles in the myocardium.¹⁰ These results suggest on the formation of a cardiac tissue with strong contraction potential. Analysis of cell area within the two types of scaffolds on days 3 and 7 revealed significantly larger cell area in the AuNPs scaffolds (Fig. 4C; $p=0.004$ on day 3, and $p<0.0001$ on day 7). Moreover, analysis of cell elongation (presented as cell aspect ratio) revealed that on day 3 and 7 cardiac cells cultured within AuNPs scaffolds had significantly higher aspect ratio than those grown in pristine scaffolds (Fig. 4D; $p=0.005$ on day 3, and $p=0.01$ on day 7). Overall these results indicate that the AuNPs encouraged cardiac cell assembly into an organized and dense tissue with a strong and anisotropic contraction potential.

Finally, we were interested to assess the potency of AuNPs scaffolds to induce the assembly of a functional cardiac tissue. In an attempt to improve heart function after MI an engineered cardiac patch should be able to generate a strong contraction force.¹⁸ Analysis of tissue contraction rates revealed significantly higher rates in tissues cultured

within the AuNPs scaffolds as compared to pristine scaffolds (Fig. 4E, and supplementary movies 1 and 2; $p= 0.004$). To evaluate the contraction force that the tissues can generate, the longitude change of the cardiac patches was measured on day 7. Cardiac tissues cultured within AuNPs scaffolds generated significantly stronger contraction forces as compared to the tissues grown within the pristine scaffolds (Fig. 4F, and supplementary movies 1 and 2; $p= 0.03$). Based on previous studies we hypothesized that AuNPs will induce superior cell electrical coupling, leading to synchronous contraction of the entire tissue.^{11, 20} To investigate this, cardiac constructs were subjected to external electrical field, increasing in increments of 0.1 V. We Excitation threshold was defined as the minimum voltage needed to induce synchronous contractions of the entire patch at the defined frequency (higher than the normal contraction rate). Fig. 4G revealed that cardiac tissues grown within AuNPs scaffolds reacted to significantly lower electrical fields compared to those grown in pristine scaffolds ($p= 0.02$). Overall, our results indicated on the superior function of cardiac tissues cultured within coiled fiber scaffolds incorporated with AuNPs.

Conclusions

In this article we report on the incorporation of AuNPs to coiled fiber scaffolds for cardiac tissue engineering. The structure of the electrospun fibers resembled that of the coiled perimysial fibers present in the native heart matrix, allowing proper contraction and relaxation of the myocardium. The addition of AuNPs to the scaffolds induced a quick formation of elongated and aligned cardiac tissues with morphology resembling

that of cardiac cell bundles *in vivo*. Furthermore, tissues engineered within AuNPs-coiled fiber scaffolds exhibited superior function. We believe that the reported technology can be used for engineering more functional cardiac tissues within various types of biomaterial scaffolds.

Experimental

Electrospinning

PCL (17.5% w/v, Mn 80,000, Sigma-Aldrich, St. Louis, MO) was dissolved in DCM and DMF in a ratio of 1:1. A syringe pump (Harvard apparatus, Holliston, MA) was used to deliver the polymer solution through a stainless steel 20G capillary at a rate of 0.5 mL/h. A high voltage power supply (Glassman high voltage Inc., Whitehouse Station, NJ) was used to apply a 17.5 kV potential between the capillary tip and the grounded aluminum collector placed 15 cm away. The obtained fibers were examined under a light microscope to verify coiled morphology and then air-dried for 48-72 h to allow residual solvent to evaporate.

Gold NP preparation

Scaffolds, or single electrospun fibers were mounted in a VST e-beam evaporator. Au films (10 nm thick) were prepared by evaporation of Au (99.999%) from a tungsten boat at $1-3 \times 10^{-6}$ torr at a deposition rate of 0.5 \AA s^{-1} .

Topography and mechanical properties measurements by AFM

Topography and mechanical properties measurements were performed using a JPK research AFM (model NanoWizard III) in the force spectroscopy mode. We used

NanoSensors, PPP-NCHR-50 scanning probe, resonance frequency range of 204 – 497 kHz, force constant range of 10 – 130 N/m.

Scanning electron microscopy

Coiled-fiber scaffolds. Scaffolds were mounted onto aluminum stubs with conductive paint and sputter-coated with an ultrathin (150 Å) layer of gold in a Polaron E 5100 coating apparatus. The samples were viewed under SEM (JEOL model JSM-840A) at an accelerating voltage of 25 kV. *AuNPs coiled fibers.* Fibers were imaged without additional coating using a Quanta 200 FEG Environmental Scanning Electron Microscope (ESEM) with a field-emission gun (FEG) electron source. Imaging was carried out under low vacuum with a high tension of 20 kV and a working distance of 7.3 mm.

Cardiac cell isolation, seeding and cultivation

Cardiac cells were isolated as previously described.²⁶ Briefly, left ventricles of 0-3 day old neonatal Sprague-Dawley rats were harvested and cells were isolated using 6 cycles (30 min each) of enzyme digestion with collagenase type II (95 U/mL; Worthington, Lakewood, NJ) and pancreatin (0.6 mg/ml; Sigma-Aldrich) in Dulbecco's modified Eagle Medium (DMEM, (CaCl₂•2H₂O (1.8 mM), KCl (5.36 mM), MgSO₄•7H₂O (0.81 mM), NaCl (0.1 M), NaHCO₃ (0.44 mM), NaH₂PO₄ (0.9 mM))). After each round of digestion cells were centrifuged (600 G, 5 min) and re-suspended in culture medium composed of M-199 (Biological Industries, Beit-Haemek, Israel) supplemented with 0.6 mM CuSO₄•5H₂O, 0.5 mM ZnSO₄•7H₂O, 1.5 mM vitamin B12, 500 U/mL Penicillin and 100 mg/ml streptomycin, and 0.5% (v/v) FBS. To enrich the cardiomyocytes population, cells were suspended in culture medium with 5% FBS and pre-plated twice (30 min) to enrich

cardiomyocyte population. Following, cells were counted and seeded on the scaffolds using a single droplet. The cell-seeded constructs were cultivated at 37° C in a 5% carbon dioxide humidified incubator.

Immunostaining

Immunostaining was performed as previously described.²⁷ Cardiac cell constructs were fixed and permeabilized in 100% cold methanol for 10 min, washed three times in DMEM-based buffer and then blocked for 1 h at room temperature in DMEM-based buffer containing 2% FBS. The samples were then incubated with primary antibodies to detect α -sarcomeric actinin (1:750, Sigma-Aldrich), washed three times, and incubated for 1 h with Alexa Fluor 647 conjugated goat anti-mouse antibody (1:500; Jackson, West Grove, PA) and Alexa Fluor 488 conjugated goat anti-rabbit antibody (1:500; Jackson). For nuclei detection, the cells were incubated for 3 min with Hoechst 33258 (1:100; Sigma-Aldrich) and washed three times. Samples were visualized using a confocal microscope (Nikon Eclipse Ni).

Functional assessment

Contractions. Samples were filmed under a microscope (Nikon Eclipse Ti, inverted) for functional assessments. Longitude change during tissue contraction was analyzed using image J (NIH). Contraction rate was counted. At least 5 samples from each group were used for analyses. *Excitation threshold.* Cell constructs were placed in Tyrode's solution at 37°C between two carbon electrode rods placed 1 cm apart in a Petri dish. Constructs were stimulated with 100 ms square pulses delivered at a rate of 2 Hz, starting with an amplitude of 1 V electrical field. The amplitude was increased by 0.1 V increments.

Excitation threshold was defined as the voltage where the tissue construct started to contract synchronously at a frequency of 2 Hz.

Statistical analysis

Statistical analysis data are presented as means \pm SEM. Univariate differences between the pristine scaffold and AuNPs scaffolds were assessed with Student's t-test. All analyses were performed using GraphPad Prism version 5.00 for Windows (GraphPad Software). $p < 0.05$ was considered significant.

Acknowledgment

T.D acknowledges support from the European Union FP7 program (Marie Curie, CIG), Alon Fellowship, and the Israeli Science Foundation.

References

1. A. S. Go, D. Mozaffarian, V. L. Roger, E. J. Benjamin, J. D. Berry, M. J. Blaha, *et al.*, Heart Disease and Stroke Statistics--2014 Update: A Report From the American Heart Association, *Circulation*, 2013.
2. A. S. Go, D. Mozaffarian, V. L. Roger, E. J. Benjamin, J. D. Berry, W. B. Borden, *et al.*, Executive summary: heart disease and stroke statistics--2013 update: a report from the American Heart Association, *Circulation*, 2013, **127**(1), 143-152.
3. A. R. Williams, K. E. Hatzistergos, B. Addicott, F. McCall, D. Carvalho, V. Suncion, *et al.*, Enhanced effect of combining human cardiac stem cells and bone marrow mesenchymal stem cells to reduce infarct size and to restore cardiac function after myocardial infarction, *Circulation*, 2013, **127**(2), 213-223.
4. R. Bolli, A. R. Chugh, D. D'Amario, J. H. Loughran, M. F. Stoddard, S. Ikram, *et al.*, Cardiac stem cells in patients with ischaemic cardiomyopathy (SCIPIO): initial results of a randomised phase 1 trial, *Lancet*, 2011, **378**(9806), 1847-1857.
5. S. Fleischer and T. Dvir, Tissue engineering on the nanoscale: lessons from the heart, *Current opinion in biotechnology*, 2013, **24**(4), 664-671.
6. J. Buikema, P. van der Meer, J. P. Sluijter and I. J. Domian, Engineering Myocardial Tissue: The Convergence of Stem Cells Biology and Tissue Engineering Technology, *Stem Cells*, 2013.
7. M. A. Laflamme and C. E. Murry, Heart regeneration, *Nature*, 2011, **473**(7347), 326-335.
8. G. Vunjak-Novakovic, N. Tandon, A. Godier, R. Maidhof, A. Marsano, T. P. Martens, *et al.*, Challenges in cardiac tissue engineering, *Tissue engineering. Part B, Reviews*, 2010, **16**(2), 169-187.

9. T. Eschenhagen, A. Eder, I. Vollert and A. Hansen, Physiological aspects of cardiac tissue engineering, *American journal of physiology. Heart and circulatory physiology*, 2012, **303**(2), H133-143.
10. T. Dvir, B. P. Timko, D. S. Kohane and R. Langer, Nanotechnological strategies for engineering complex tissues, *Nature nanotechnology*, 2011, **6**(1), 13-22.
11. T. Dvir, B. P. Timko, M. D. Brigham, S. R. Naik, S. S. Karajanagi, O. Levy, *et al.*, Nanowired three-dimensional cardiac patches, *Nature nanotechnology*, 2011, **6**(11), 720-725.
12. M. Radisic, H. Park, H. Shing, T. Consi, F. J. Schoen, R. Langer, *et al.*, Functional assembly of engineered myocardium by electrical stimulation of cardiac myocytes cultured on scaffolds, *Proceedings of the National Academy of Sciences of the United States of America*, 2004, **101**(52), 18129-18134.
13. Y. Sapir, O. Kryukov and S. Cohen, Integration of multiple cell-matrix interactions into alginate scaffolds for promoting cardiac tissue regeneration, *Biomaterials*, 2011, **32**(7), 1838-1847.
14. B. Liao, N. Christoforou, K. W. Leong and N. Bursac, Pluripotent stem cell-derived cardiac tissue patch with advanced structure and function, *Biomaterials*, 2011, **32**(35), 9180-9187.
15. G. C. Engelmayr, Jr., M. Cheng, C. J. Bettinger, J. T. Borenstein, R. Langer and L. E. Freed, Accordion-like honeycombs for tissue engineering of cardiac anisotropy, *Nature materials*, 2008, **7**(12), 1003-1010.
16. T. Dvir, A. Kedem, E. Ruvinov, O. Levy, I. Freeman, N. Landa, *et al.*, Prevascularization of cardiac patch on the omentum improves its therapeutic outcome, *Proceedings of the National Academy of Sciences of the United States of America*, 2009, **106**(35), 14990-14995.
17. W. H. Zimmermann, I. Melnychenko, G. Wasmeier, M. Didie, H. Naito, U. Nixdorff, *et al.*, Engineered heart tissue grafts improve systolic and diastolic function in infarcted rat hearts, *Nature medicine*, 2006, **12**(4), 452-458.
18. R. K. Iyer, L. L. Chiu, L. A. Reis and M. Radisic, Engineered cardiac tissues, *Current opinion in biotechnology*, 2011, **22**(5), 706-714.
19. N. Bursac, Y. Loo, K. Leong and L. Tung, Novel anisotropic engineered cardiac tissues: studies of electrical propagation, *Biochemical and biophysical research communications*, 2007, **361**(4), 847-853.
20. M. Shevach, B. M. Maoz, R. Feiner, A. Shapira and T. Dvir, Nanoengineering gold particle composite fibers for cardiac tissue engineering, *Journal of Materials Chemistry B*, 2013, **1**(39), 5210-5217.
21. T. F. Robinson, M. A. Geraci, E. H. Sonnenblick and S. M. Factor, Coiled perimysial fibers of papillary muscle in rat heart: morphology, distribution, and changes in configuration, *Circulation research*, 1988, **63**(3), 577-592.
22. P. J. Hanley, A. A. Young, I. J. LeGrice, S. G. Edgar and D. S. Loiselle, 3-Dimensional configuration of perimysial collagen fibres in rat cardiac muscle at resting and extended sarcomere lengths, *The Journal of physiology*, 1999, **517** (Pt 3), 831-837.
23. S. Fleischer, R. Feiner, A. Shapira, J. Ji, X. Sui, H. Daniel Wagner, *et al.*, Spring-like fibers for cardiac tissue engineering, *Biomaterials*, 2013, **34**(34), 8599-8606.
24. T. Cohen-Karni, K. J. Jeong, J. H. Tsui, G. Reznor, M. Mustata, M. Wanunu, *et al.*, Nanocomposite gold-silk nanofibers, *Nano letters*, 2012, **12**(10), 5403-5406.
25. J. O. You, M. Rafat, G. J. Ye and D. T. Auguste, Nanoengineering the heart: conductive scaffolds enhance connexin 43 expression, *Nano letters*, 2011, **11**(9), 3643-3648.

26. T. Dvir, N. Benishti, M. Shachar and S. Cohen, A novel perfusion bioreactor providing a homogenous milieu for tissue regeneration, *Tissue engineering*, 2006, **12**(10), 2843-2852.
27. T. Dvir, O. Levy, M. Shachar, Y. Granot and S. Cohen, Activation of the ERK1/2 cascade via pulsatile interstitial fluid flow promotes cardiac tissue assembly, *Tissue engineering*, 2007, **13**(9), 2185-2193.

Fleischer et al. Coiled fiber scaffolds embedded with gold nanoparticles improve the performance of engineered cardiac tissues

Figure legends

Figure 1. Schematic representation of the study.

Figure 2. Native and synthetic coiled fibers. (A) SEM image of the coiled perimysial fibers in a decellularized heart. (B) ESEM image of electrospun coiled fiber embedded with AuNPs. (C, D) SEM images of coiled fiber scaffolds. (E) ESEM image of the AuNPs embedded on the synthetic fiber. (F) EDX spectrum of AuNPs coiled fibers. Bars: A, B and D- 20 μm , C- 50 μm , E- 250 nm.

Figure 3. Topography and mechanical properties by AFM. (A) Topography of a coiled fiber supplemented with AuNPs. (B) Topography of a non-modified coiled fiber. (C) Analysis of Young's modulus by AFM.

Figure 4. Cardiac tissue organization and function. (A, B) Cardiac sarcomeric actinin immunostaining on day 7. Actinin – pink, nuclei – blue. (A) Cardiac tissue engineered within pristine scaffolds. (B) Cardiac tissue engineered within AuNPs scaffolds. (C) Cardiomyocyte area on day 3 and 7. (D) Cardiomyocyte aspect ratio on days 3 and 7. (E-G) Engineered tissue function. (E) Contraction rate on day 7. (F) Longitude change of the cell constructs on day 7. (G) Excitation threshold (ET) on day 7. Bars: left and right figures- 50 μm and 20 μm , respectively.

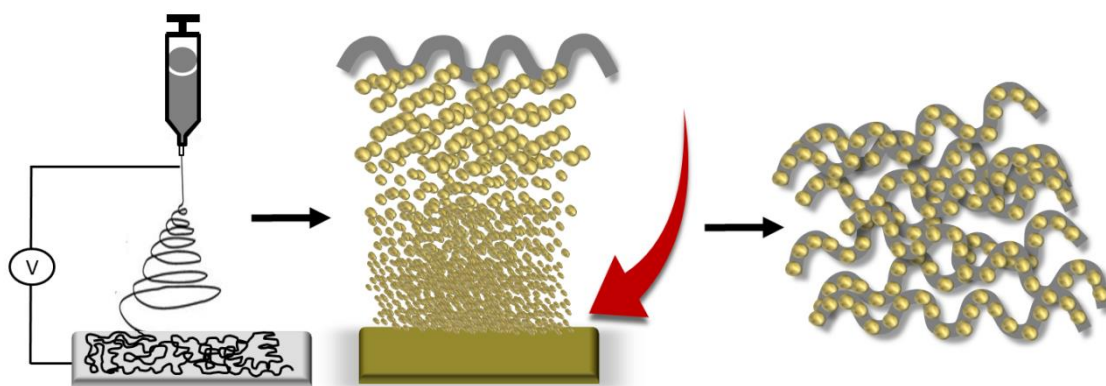


Figure 1

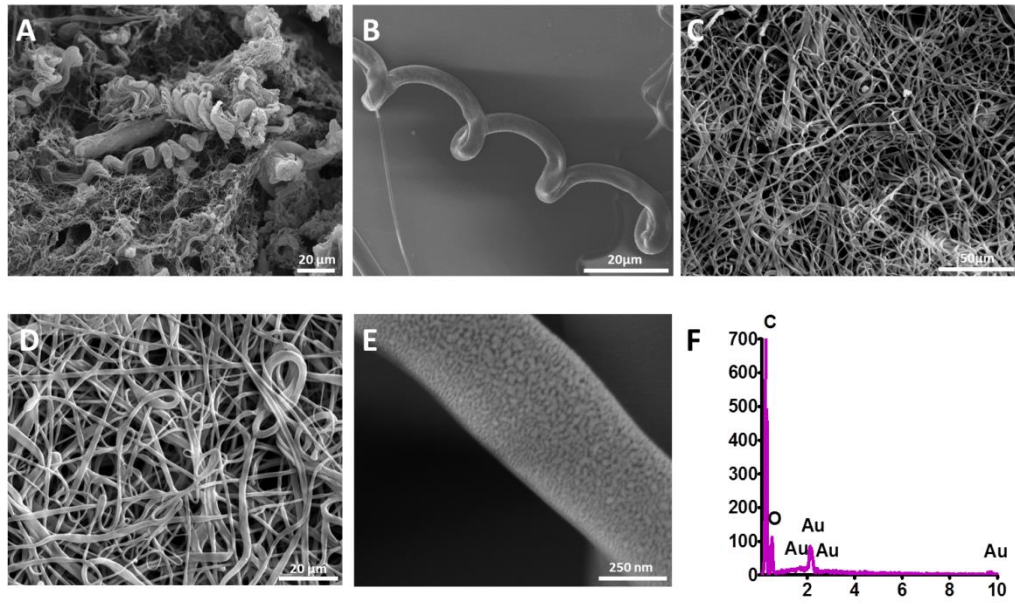


Figure 2

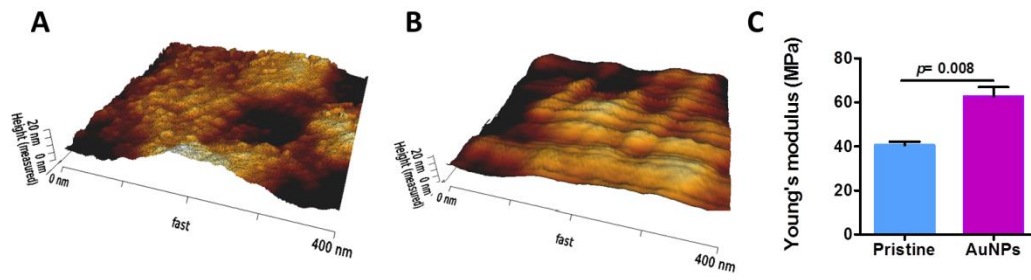


Figure 3

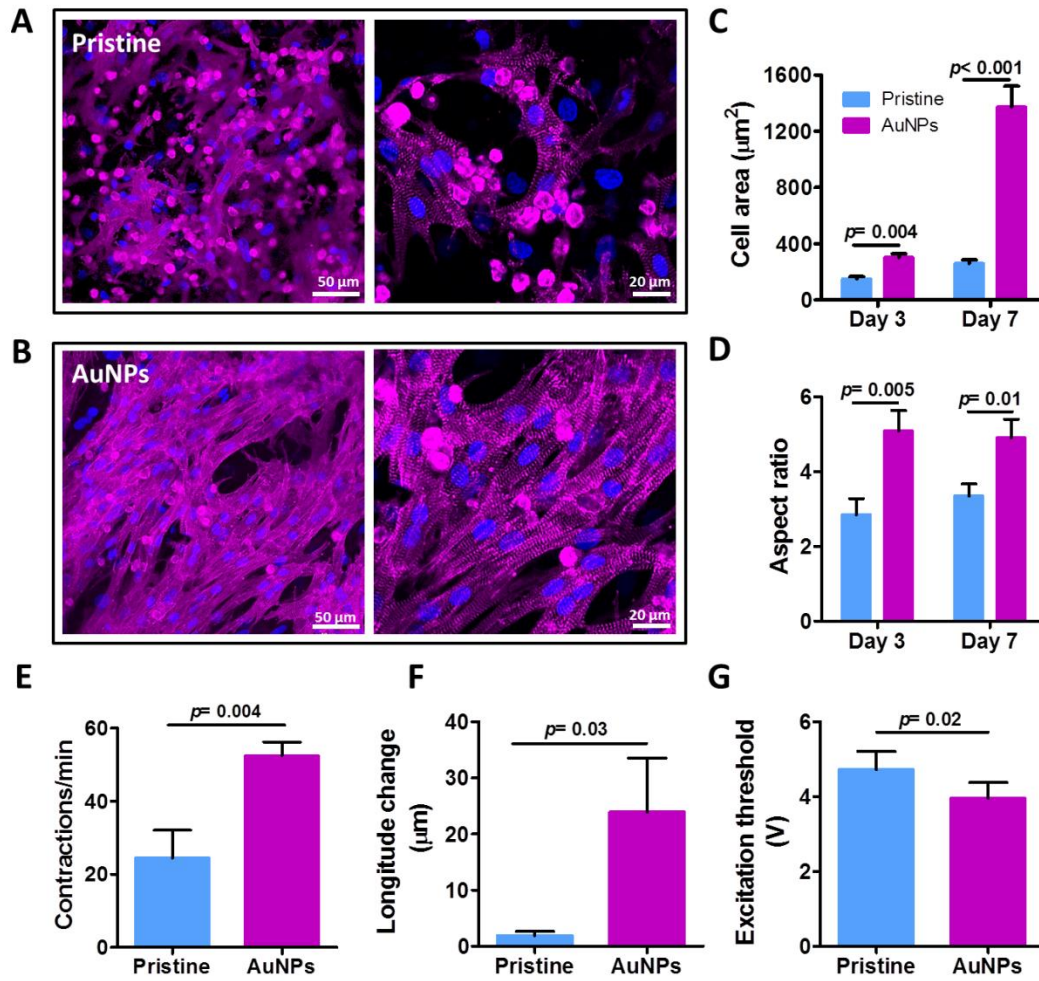


Figure 4